Published in final edited form as:
Am J Physiol Lung Cell Mol Physiol. 2007 February ; 292(2): L519–L528. doi:10.1152/ajplung.00312.2006.

IL-23 mediates inflammatory responses to mucoid *Pseudomonas aeruginosa* lung infection in mice

Patricia J. Dubin and **Jay K. Kolls**
Division of Pediatric Pulmonology, Children's Hospital of Pittsburgh, Pittsburgh, Pennsylvania

Abstract

Patients with cystic fibrosis (CF) develop chronic *Pseudomonas aeruginosa* lung infection with mucoid strains of *P. aeruginosa*; these infections cause significant morbidity. The immunological response in these infections is characterized by an influx of neutrophils to the lung and subsequent lung damage over time; however, the underlying mediators to this response are not well understood. We recently reported that IL-23 and IL-17 were elevated in the sputum of patients with CF who were actively infected with *P. aeruginosa*; however, the importance of IL-23 and IL-17 in mediating this inflammation was unclear. To understand the role that IL-23 plays in initiating airway inflammation in response to *P. aeruginosa*, IL-23p19$^{-/-}$ (IL-23 deficient) and wild-type (WT) mice were challenged with agarose beads containing a clinical, mucoid isolate of *P. aeruginosa*. Levels of proinflammatory cytokines, chemokines, bacterial dissemination, and inflammatory infiltrates were measured. IL-23-deficient mice had significantly lower induction of IL-17, keratinocyte-derived chemokine (KC), and IL-6, decreased bronchoalveolar lavage (BAL) neutrophils, metalloproteinase-9 (MMP-9), and reduced airway inflammation than WT mice. Despite the reduced level of inflammation in IL-23p19$^{-/-}$ mice, there were no differences in the induction of TNF and interferon-γ or in bacterial dissemination between the two groups. This study demonstrates that IL-23 plays a critical role in generating airway inflammation observed in mucoid *P. aeruginosa* infection and suggests that IL-23 could be a potential target for immunotherapy to treat airway inflammation in CF.

Keywords

cytokines; bronchiectasis; neutrophil; CXC chemokine

Pseudomonas aeruginosa is a gram-negative, aerobic bacillus that is normally found in the environment. Although it does not cause pulmonary infections in immunocompetent individuals, *P. aeruginosa* causes chronic lung infection in individuals with cystic fibrosis (CF), resulting in significant morbidity and mortality. The immune response to *P. aeruginosa* pulmonary infection has been described and is characterized by a vigorous neutrophil response, elevated neutrophil elastase activity, leukotriene B_4, IL-1, IL-6, IL-8, and TNF, and decreased levels of IL-10 (2,3,5,7,25,26,28). Moreover, in addition to this local cytokine/chemokine response, many patients have evidence of adaptive immune responses such as antibodies or T cell proliferative responses against specific *P. aeruginosa* antigens (4,8,16,20,30). Matrix metalloproteinase (MMP) activity is also elevated (32,34) in CF and may explain the bronchiectasis observed (31,41). However, these observations have not been synthesized into an immunological model for the host response to *P. aeruginosa* infection in CF.

Address for reprint requests and other correspondence: J. K. Kolls, Children's Hospital of Pittsburgh, Suite 3765, 3705 Fifth Ave., Pittsburgh, PA 15213 (jay.kolls@chp.edu).

The IL-12 family of heterodimeric cytokines, including IL-12p70 and IL-23, are master regulators of the transition between innate and adaptive immunity by controlling T helper type 1 (Th1) and "ThIL-17" responses, respectively (1,21,22). IL-23, which has been recently described, is more strongly identified with a ThIL-17 phenotype, whereas IL-12 drives the Th1 response to infection (1,13,14,21,22,29). IL-17 induction has been shown to induce production of CXC chemokines, which are critical in the recruitment and activation of neutrophils (12, 18,40); IL-17 has also been shown to induce matrix MMPs that are linked to cartilage destruction (23). Although the IL-23/IL-17 proinflammatory axis has been more extensively described in models of experimental autoimmune encephalitis (9) and collagen-induced arthritis (27), there is a growing body of literature describing the importance of IL-23 and IL-17 family members in respiratory inflammatory responses to infectious agents.

Interestingly, *Bordetella pertussis*, a significant cause of bronchiectasis before widespread vaccination (11), elicits a potent IL-23 response as opposed to inducing IL-12p70 (37). The host inflammatory response to *Klebsiella pneumoniae* pulmonary infection is also mediated by IL-23 (12,13), and mycobacterial infection has been studied in the context of IL-23 and IL-17 (17). Our group has also recently demonstrated elevated levels of IL-23p19, IL-17A, and IL-17F in the sputum of adult CF patients colonized with *P. aeruginosa* undergoing a pulmonary exacerbation (24). Taken together, these findings suggested that IL-23 and IL-17 could be critical in mediating the inflammatory response to *P. aeruginosa* infection in the lung and led to the hypothesis that *P. aeruginosa* infection in the airways leads to the induction of IL-23 in the lung and IL-23 regulates the subsequent induction of IL-17 and CXC chemokines, neutrophil recruitment to the airways, and possible upregulation of MMPs. We tested this hypothesis by using a well-established murine model of *P. aeruginosa* lung infection that has been previously used in screening candidate anti-inflammatory medications to treat airway inflammation in CF (39).

Wild-type (WT) and IL-23-deficient mice were infected with agarose beads laden with a clinical, mucoid strain of *P. aeruginosa* to model the airway infections seen in CF. Inflammatory parameters that are critical to the IL-23/IL-17 inflammatory axis were measured and reported at time points appropriate to their elaboration. These studies showed that the components of IL-23, both IL-23p19 and IL-12p40, are induced at the same time and precede the elevation in IL-17. Moreover, WT mice demonstrated higher levels of the proinflammatory cytokines and chemokines involved in neutrophil emigration and MMP-9 compared with IL-23-deficient mice. IL-23p19$^{-/-}$ mice also had significantly less airway inflammation based on histological scoring of lung sections. Despite this reduction in airway inflammation, there were no differences in pulmonary bacterial load or dissemination of bacteria between the two groups, demonstrating that, although IL-23 regulates airway inflammation, it is not required for control of bacterial infection in this model.

MATERIALS AND METHODS

Mice

Specific pathogen-free C57BL/6 (National Cancer Institute, Frederick, MD) were used in all experiments as the WT mice. IL-23p19$^{-/-}$ (backcrossed to C57BL/6 background to 10 generations using speed congenics) were obtained from Genentech and bred in the Children's Hospital of Pittsburgh animal care facilities. The IL-23p19$^{-/-}$ mice were confirmed genetically by PCR. Male, 8- to 10-wk-old C57BL/6 and IL-23p19$^{-/-}$ mice were used in this study. All mice were housed in specific pathogen-free rooms within the animal care facilities of Children's Hospital of Pittsburgh under protocols reviewed and approved by the Animal Research and Care Committee. Mice were provided with water and food ad libitum and received 12-h light/dark cycles until the date of the experiment.

P. aeruginosa strain

Dr. Anna van Heeckeren (Case Western Reserve University Cystic Fibrosis Center, Cleveland, OH) generously provided the mucoid clinical strain PA M57–15 of *P. aeruginosa*. The bacteria were maintained in glycerol stocks and maintained at −80°C.

P. aeruginosa agarose beads and inoculation of mice

Agarose beads were prepared as previously outlined by van Heeckeren et al. (38) and resulted in an end concentration of 1×10^5 colony-forming units (CFU)/50 μl PBS. Briefly, PA M57–15 was grown to late log phase in tryptic soy broth (Difco, Detroit, MI), and a 5-ml aliquot was mixed with sterile agarose and subsequently mixed into mineral oil under temperature-controlled conditions. The mineral oil was stirred and cooled over a total period of 16 min, and the resulting agarose beads were washed with sterile 0.5% deoxycholic acid (SDC) in PBS, 0.25% SDC, and four subsequent washes with sterile PBS for removal of the mineral oil and detergent. Microscopic quantification of bead diameters was completed for quality control and serial dilutions of beads were processed and cultured on tryptic soy agar (TSA) plates to confirm the inoculum. PA M57–15-laden agarose beads were stored overnight at 4°C prior to use.

For inoculation of the PA M57–15-laden beads, the mice were anesthetized using isoflurane delivered by nose cone. The mice were positioned on a rodent procedure board, the site prepped with alcohol and betadine, and the trachea exposed. Using a 22-gauge Abbocath-Tangiocatheter (Abbott Laboratories, Dublin, Ireland), the trachea was cannulated, the catheter tip was directed to the right main bronchus, and the beads were introduced into the right lung at an average inoculum of 1×10^5 CFU/50 μl per mouse (38). Mice were monitored, allowed to recover, and transferred to a clean box with food and water ad libitum until killed. The average procedure-related mortality was 10% and accounts for the disparity in numbers in comparative experimental groups.

Structure of experiments

In the outlined studies, WT and IL-23p19$^{-/-}$ mice were treated with sterile control agarose beads or PA M57–15-laden agarose beads. These mice were killed at 0, 3, 5, and 7 days, and lung tissue and bronchoalveolar lavage (BAL) fluid were processed for analysis. Lavage was performed on 8–10 mice per time point, allowing analysis for cell counts and differential; BAL samples from the first five mice in each group were further processed for cytokine and chemokine analysis. Lung tissue was obtained and processed for all time points for *1*) histological analysis, *2*) RNA for real-time PCR, or *3*) homogenate for protein analysis and bacterial counts. Four to five mice were allocated for each of the three tissue groups at each time point. The difference in numbers among groups is a result of the procedure-related mortality.

Because of the large number of mice treated in these studies, individual experiments were structured to include combinations of two of the three tissue groups for all time points, and different combinations were run to verify agreement of the findings. Overall, the different tissue groups and BAL analyses were replicated three times for the mice treated with PA M57–15-laden beads and two times for the mice treated with control beads.

Additional studies ($n = 3$ per group) at earlier time points of 0, 6, 24, and 48 h after bead inoculation were conducted to clarify the chronology of IL-23p19 induction and IL-17 production. These studies were specifically targeted to obtain mRNA for analysis by TaqMan and BAL for IL-17 protein assessment.

Bronchoalveolar lavage and cell count and differential

Cells and BAL fluid were obtained from mice killed using CO_2 asphyxiation. Briefly, lungs were lavaged with 1 ml of prewarmed (37°C) calcium-and magnesium-free PBS supplemented with 0.6 mM EDTA through a 22-gauge bead-tipped feeding needle introduced into the trachea. BAL fluid was centrifuged at 300 *g*, and supernatant was stored at −80°C for later use in Luminex assays and enzyme-linked immunosorbent assays (ELISA). The cell pellet from BAL fluid was resuspended in 1 ml of PBS. The cell count was completed using the Z1 particle counter (Beckman Coulter, Fullerton, CA). Cell differential was quantified using the Shandon Cytospin 4 (Thermo Electron, Cheshire, UK) by counting a minimum of 100 cells per sample.

Luminex assays and ELISA

The chemokines macrophage inflammatory protein-1α(MIP-1α), IFN-γ-inducible protein 10 (IP-10), and keratinocyte-derived chemokine (KC), the cytokines IL-6, IFN-γ, and TNF-α, and MMP-9 were measured by Luminex (LINCOplex; LINCO Research, St. Charles, MO) on the Bioplex analyzer (Bio-Rad, Hercules, CA) according to the manufacturer's protocol. IL-17, IL-12p40, and LPS-induced CXC chemokine (LIX) ELISAs were performed according to the manufacturer's protocol (R&D Systems, Minneapolis, MN) on BAL. IL-23 was not assessed at the protein level due to inconsistencies in the results obtained with commercially available reagents, and IL-23 quantitation was performed by real-time PCR.

Real-time PCR

For total RNA extraction, lungs were homogenized in 2 ml of TRIzol reagent (Invitrogen Life Technologies, Carlsbad, CA) using an Ultra Turrax T8 homogenizer (IKA, Wilmington, NC) and processed according to the manufacturer's protocol. For real-time PCR, 1 μg of total RNA was reverse-transcribed to cDNA using TaqMan reverse transcription reagents (Applied Biosystems, Foster City, CA) on the iCycler thermocycler (Bio-Rad). For real-time PCR, gene-specific primers and dual-labeled probe sequences for the IL-23 specific subunit, IL-23p19 (12), were as follows (primer, primer, probe): IL-23p19, 5′-TGGCTGTGCCTAGGAGTAGCA-3′, 5′-TTCATCCTCTTCTTCTCTTAGTAGATTCATA-3′, 5′-CTCTG-CATGCTAGCCTGGAAC-3′. All samples were normalized to 18S rRNA content using TaqMan ribosomal control reagents (Applied Biosystems). Data are expressed as transcript copy numbers per nanogram of 18S rRNA.

Lung histology

In certain experiments, the lungs from mice in each group were inflated with 10% neutral-buffered formalin and embedded in paraffin, sectioned and stained with hematoxylin and eosin (Histo-Scientific Research Laboratories), and histologically scored. Histology scoring consisted of a five-point system as outlined in Table 1. Ten fields were evaluated from three to five mice per group, per time point, at low power (×50). Scoring of lung sections was performed blindly by one of the co-investigators (J. K. Kolls).

Homogenate for protein and bacterial load and dissemination measurements

In other experiments, the lungs from mice in each group were removed at each time point from the chest via sterile excision and homogenized in 1 ml of sterile PBS using an Ultra Turrax T8 homogenizer (IKA). The homogenizer was disinfected between each sample using 70% ethanol and rinsed of the ethanol with sterile water to avoid inhibition of bacterial growth in the subsequent sample. The samples were serially diluted with sterile PBS and cultured on TSA plates overnight at 37°C. Bacterial colony counts from each animal were counted, averaged, and compared between groups. In addition to comparing average bacterial load per group, the number of animals that were positive were counted and compared as percents for

each animal group and time point. For protein measurements (KC and MMP-9), the sample was frozen for later analysis by LINCOplex.

The spleens were also removed from mice in each group at each time point and homogenized in 1 ml of sterile PBS as described for the lungs. Serial dilutions were also plated and analyzed for colony counts. In addition to assessing bacterial dissemination by comparing average bacterial colony counts for the WT and IL-23p19$^{-/-}$ mice, the number of animals that demonstrated bacterial growth were counted and compared as percents for each animal group and time point.

Statistical analysis

Data were analyzed using GraphPad Prism 4 statistical software (San Diego, CA). Comparisons among multiple groups or nonparametric data were made with analyses of variance. The Scheffé test was the post hoc test used. Significance was accepted at a P value of <0.05. Data points were graphed as mean ± SE.

RESULTS

IL-23 elaboration after *P. aeruginosa* agarose bead infection

IL-23p19 mRNA induction was measured via real-time PCR at *days 0*, *3*, *5*, and *7*. Comparisons were made between WT and IL-23-deficient mice and demonstrated elevated levels of IL-23p19 message on *days 3* and *5* of infection ($P < 0.05$) with some detectable IL-23p19 persisting at *day 7* for the WT mice (Fig. 1*A*). IL-23p19$^{-/-}$ mice, as expected, did not express measurable IL-23p19 (Fig. 1*A*). There was no basal expression of IL-23p19 transcripts in uninfected lung or in lungs challenged with sterile control agarose beads. Measurement of IL-23 at the protein level was attempted; however, PA M57–15 infection resulted in significantly elevated IL-23 protein levels that were not reliably quantifiable; the currently available ELISA shows apparent cross-reactivity with IL-12p40, which can be found as a constituent of IL-12, IL-23, or as p40 monomers or dimers (data not shown). IL-12p40, which was measured at the protein level, was not significantly different between the infected IL-23p19$^{-/-}$ and WT mice at any time point and was elevated above baseline and control mice at *day 3* in both groups (Fig. 1*B*). The IL-12p40 levels were not significantly different between the IL-23p19$^{-/-}$ and WT control mice. IL-12p70 levels were less than 15 pg/ml at each time point analyzed (data not shown).

IL-17 protein levels in BAL fluid showed similar kinetic profiles as IL-23p19 mRNA again with peak on *day 3* of infection (Fig. 2). Because IL-23 production would need to precede IL-17 elaboration if it were responsible for IL-17 induction, we realized that to test the proposed hypothesis, we would need to conduct additional experiments at earlier time points to have better resolution of the chronology of the events in question. As a result, we conducted additional experiments, and these studies demonstrated an elevation of IL-23p19 mRNA as early as 6 h after infection (1,260 copies of IL-23p19 per nanogram of 18S rRNA); thus there is acute expression of IL-23 even in this chronic model of infection. Furthermore, this upregulation of IL-23 production precedes IL-17 induction. Again, in these studies, there was no appreciable induction of IL-17 in mice treated with control beads.

Cytokine, chemokine, and MMP-9 levels

IL-17 was significantly increased in the WT BAL at *day 3* compared with baseline BAL values at *day 0* and IL-23p19$^{-/-}$ BAL at all time points ($P < 0.05$); IL-17 levels were undetectable in the infected IL-23p19$^{-/-}$ BAL and in the WT and IL-23p19$^{-/-}$ control BAL (Fig. 2). Measured chemokine levels are reported for *day 5* of infection based on the kinetics of the IL-23/IL-17 proinflammatory axis. IL-23p19$^{-/-}$ mice had significantly lower levels of KC in lung

homogenate compared with WT mice ($P < 0.05$, Fig. 3*A*); KC in mice given control beads was <50 pg/mg protein and was not significantly different between WT and IL-23p19$^{-/-}$ mice.

We also observed reduction of MIP-1α and IP-10 (Fig. 3, *B* and *C*) in the BAL fluid of IL-23p19$^{-/-}$ mice compared with WT mice on *day 5* of bead infection ($P < 0.05$). There was no detectable production in the WT and IL-23p19$^{-/-}$ controls. LIX was elevated in the BAL of IL-23p19$^{-/-}$ mice compared with WT mice at *day 5* ($P < 0.05$, Fig. 3*D*). Total matrix MMP-9 was significantly lower in the lung homogenate of IL-23p19$^{-/-}$ mice compared with WT mice ($P < 0.05$, Fig. 3*E*). In addition, the WT infected mice demonstrated significantly higher MMP-9 levels than the WT controls, and there was no significant difference between WT and IL-23p19$^{-/-}$ control mice.

In addition, there were significantly lower levels of IL-6 in the BAL fluid of IL-23p19$^{-/-}$ mice compared with WT mice on *day 5* of infection ($P < 0.05$, Fig. 4*A*); IL-6 levels were <15 pg/ml in mice receiving control beads; the IL-6 in WT infected mice was significantly increased over WT control, and there was no significant difference between WT and IL-23p19$^{-/-}$ controls. Despite the reduction of cellular inflammation and chemokines witnessed in IL-23p19$^{-/-}$ mice, the proinflammatory cytokines interferon-γ (Fig. 4*B*) and TNF-α (Fig. 4*C*) were similarly induced above sterile bead controls in both WT and IL-23p19$^{-/-}$ mice ($P < 0.05$). There was no detectable interferon-γ or TNF-α in the WT or the IL-23p19$^{-/-}$ controls.

BAL inflammatory cell counts

Airway inflammation was assessed by enumerating inflammatory cells in BAL fluid. Both WT and IL-23p19$^{-/-}$ mice had similar levels of macrophages prior to infection, constituting nearly 100% of all cells in BAL fluid (Fig. 5, *A* and *B*). The absolute macrophage counts in the BAL of WT and IL-23p19$^{-/-}$ mice were similar at *days 3* and *5*, whereas the absolute macrophage count was significantly higher in the IL-23p19$^{-/-}$ BAL on *day 7*. Despite an elevation of absolute numbers of macrophages, both WT and IL-23p19$^{-/-}$ mice had significant declines in the percentage of macrophages in BAL by *day 3*, with the percentage of macrophages increasing toward preinfection levels on *days 5* and *7* for both IL-23p19$^{-/-}$ and WT mice (Fig. 5*A*). However, the percentage of macrophages in the IL-23p19$^{-/-}$ BAL increased more than in the WT and led to a statistically significant difference between IL-23p19$^{-/-}$ and WT mice ($P < 0.05$, Fig. 5*B*). Absolute and percent macrophages in both control groups never differed significantly from each other or from baseline.

The decrease in percentage of macrophages was accompanied by a corresponding increase in the numbers of recruited neutrophils in the BAL on *day 3* (Fig. 5, *C* and *D*). In contrast to WT mice, and consistent with the previously mentioned increase in percentage of macrophages in the IL-23p19$^{-/-}$ mice on *days 5* and *7*, the percentage of neutrophils was significantly lower in IL-23p19$^{-/-}$ mice on *days 5* and *7* of infection (Fig. 5*D*). The absolute number of neutrophils, however, was not reduced in the IL-23p19$^{-/-}$ mice compared with *day 3*, but was significantly less than in the WT mice ($P < 0.05$, Fig. 5*D*). This reduced recruitment of neutrophils in the IL-23-deficient mice compared with WT mice corresponds with the lower levels of induced chemokines (KC, MIP1-α, and IP-10; Fig. 3). Absolute and percent neutrophils in both WT and IL-23p19$^{-/-}$ control groups never differed significantly from each other or from baseline.

Tissue histology

Figure 6 shows representative lung histology at *days 3*, *5*, and *7* after treatment for both WT and IL-23p19$^{-/-}$ infected mice. WT mice showed robust neutrophilic airway inflammation on *day 3* (Fig. 6, *a* and *c*), which was significantly attenuated in IL-23p19$^{-/-}$ mice (Fig. 6, *b* and *d*). Moreover, peribronchial inflammation increased from *day 3* to *days 5* and *7* in WT mice (Fig. 6, *e* and *g*, and *i* and *k*, respectively), whereas IL-23p19$^{-/-}$ mice showed less prominent

focal areas of peribronchial inflammation (Fig. 6, *f* and *h*, and *j* and *l*). Reduced intraluminal and peribronchial inflammation was also confirmed using a quantitative scoring system, which is outlined in Table 1. Based on this scoring system, the intraluminal and peribronchial infiltrates were significantly increased in WT vs. IL-23p19$^{-/-}$ mice and significantly greater in infected WT mice than control WT mice. There was no significant difference between WT and IL-23p19$^{-/-}$ control mice (Fig. 7, *A* and *B*).

Bacterial load and dissemination

Bacterial load in the lungs (Fig. 8*A*) was not significantly different for the WT and IL-23p19$^{-/-}$ mice at *days 3*, *5*, or *7*. In addition, the percent of mice positive for bacterial growth in the lung (Fig. 8*B*) was not significantly different between WT and IL-23p19$^{-/-}$ mice at each time point measured. Dissemination of *P. aeruginosa*, as measured by detectable CFU in the spleen, was not significantly different between the WT and IL-23p19$^{-/-}$ mice either by absolute bacterial CFU in the spleen or the percent positive mice (data not shown). In addition, there was no detectable CFU for any of the control groups.

In summary, there were no significant differences between WT and IL-23p19$^{-/-}$ mice treated with control beads at any of the time points when considering the cytokines, chemokines, inflammatory cell counts, or histological scoring reported. There were significantly higher levels of all the cytokines and chemokines in the WT vs. IL-23p19$^{-/-}$ mice treated with PA M57–15-laden beads except for TNF-α and IFN-γ, which were not significantly different, and LIX, which was significantly higher in the IL-23p19$^{-/-}$ mice. Neutrophil counts and histological scoring were also higher in the WT vs. IL-23p19$^{-/-}$ mice at the later time points. Comparing WT mice treated with control beads and those treated with PA M57–15-laden beads, there were significant differences in neutrophil counts, histological scores, and all of the cytokines and chemokines assayed. Unless stated, the IL-23p19$^{-/-}$ mice that were administered PA M57–15 beads did not differ from baseline or those IL-23p19$^{-/-}$ mice treated with control beads.

DISCUSSION

P. aeruginosa is an opportunistic pathogen that causes significant morbidity and mortality in individuals with CF by causing chronic air space infection. The immunological mechanisms for this are not well understood, but the common final pathway of florid neutrophilic infiltrate in the airways with subsequent airway damage and bronchiectasis is well described in the literature. We hypothesized that IL-23 and IL-17, two proinflammatory cytokines that are capable of inducing CXC chemokines and neutrophil recruitment, are critical to neutrophil recruitment in response to *P. aeruginosa* airway infection.

This study demonstrates that the inflammatory response in a murine model of mucoid *P. aeruginosa* airway infection is dependent on IL-23, which, in turn, induces IL-17 production and the subsequent local production of cytokines and chemokines that are critical to airway inflammation (18). Although it is true that gene expression does not necessarily result in protein production, IL-23p19 production is tightly regulated. Moreover, IL-17 in response to extracellular gram-negative bacteria is dependent on IL-23 (12), and the fact that IL-23p19$^{-/-}$ is induced by *P. aeruginosa* beads, along with the fact that IL-23p19$^{-/-}$ have diminished IL-17, strongly suggests that functional IL-23 is produced in this model. In this study, KC, MIP-1α, and IL-6 production were also identified as IL-23-dependent.

LIX production, however, was significantly higher in the IL-23p19$^{-/-}$ mice compared with WT mice. Induction of this chemokine may explain the non-IL-23/IL-17-dependent neutrophil recruitment seen in the IL-23-deficient mice. Interestingly, LIX production has been shown to be defective when IL-23p19$^{-/-}$ are challenged with *K. pneumoniae*, and LIX expression is

rescued when IL-17 is replaced at physiological levels, demonstrating that IL-23 and IL-17 are critical to LIX induction in *K. pneumoniae* pulmonary infection. The differences in the LIX expression in these two models may relate to differences in pattern recognition receptors activated by these two pathogens or the relative differences in virulence of these two gram-negative bacteria. Of note also, although IL-17 is sufficient for induction of LIX in a model of periodontal disease, IL-17 is not necessary for its induction (33).

In considering the contributions of IL-23 to inflammation, the role of IL-12, IL-12p40 homodimers, and IL-12p40 monomers must also be considered. From a historical perspective, IL-23 has only been recently described, and the significance of constitutive expression and release of IL-12p40 as a monomer/homodimer were unrecognized until recently. Many inflammatory effects measured by elevations in IL-12p40 were often attributed to IL-12 (IL-12p70) without the recognition that these effects might be due to IL-23, IL-12p40 monomers, or IL-12p40 homodimers. For this reason, we measured IL-12p70 and IL-12p40 by ELISA to determine if there were significant levels or significant differences in levels produced by the WT or IL-23p19$^{-/-}$ mice. As noted, IL-12p70 levels were never more than 15 pg/ml and, more often than not, undetectable. This effectively rules out a contribution of IL-12 to the inflammatory effects reported in this study.

In addition, constitutive production of IL-12p40 was detected in both IL-23p19$^{-/-}$ and WT mice, and elevation was noted for both groups at *day 3*. Based on our current understanding of IL-12 family cytokines, we must attribute the IL-12p40 measured in WT mice to IL-23, IL-12p40 homodimers, and IL-12p40 monomers. For the IL-23p19$^{-/-}$ mice, we must attribute the IL-12p40 levels to IL-12p40 monomers and homodimers. Because the action of IL-12p40 is to bind the IL-12 receptor and competitively inhibit IL-12p70 biological activity (15), and there is no significant IL-12p70 production, based on our current understanding of IL-12p40 function, it is unlikely that IL-12p40 accounts for the reduced inflammation observed in IL-23p19$^{-/-}$ mice.

Because of the induction of IL-23p19 and IL-17 in infected WT mice with subsequent elevation in CXC chemokines and neutrophil recruitment, combined with the significantly impaired neutrophil recruitment in IL-23-deficient mice, we conclude that IL-23 is a critical proximal proinflammatory cytokine that mediates the neutrophilic recruitment and infiltration in this model of airway inflammation mediated by a mucoid strain of *P. aeruginosa*. These findings suggest that the elevated IL-23 and IL-17 levels observed during active pulmonary infection in a cohort of individuals with CF are not coincidental and may be critical to the neutrophilic inflammation. Because airway destruction and bronchiectasis are likely mediated by both bacterial and neutrophil proteases (6,35,36), antagonizing host inflammatory responses may be beneficial in preserving airway integrity.

In fact, two trials in CF patients, one with prednisone (10) and one with ibuprofen (19), support that targeted anti-inflammatory therapy can preserve lung function even in the setting of chronic, mucoid *P. aeruginosa* infection. Unfortunately, the chronic use of steroids and nonsteroidal anti-inflammatory agents can result in significant systemic side effects that make adherence to both therapies difficult for patients.

Critical to any immunomodulatory strategy is minimization of the risk of serious systemic side effects. Of note, although the loss of IL-23 function did significantly downregulate neutrophil recruitment and total levels of MMP-9, the lack of functional IL-23 did not result in elevated bacterial load in the lung or an increase in bacterial dissemination to the spleen. This suggests that the elimination of IL-23 could help curb host-mediated inflammatory activity and airway damage but would not be so immunosuppressive as to potentiate generalized dissemination of the *P. aeruginosa* infection. The additional observation that IL-23 is not essential for host

control of mycobacteria (17), which commonly causes infections in the lungs of patients with CF, is also reassuring when considering IL-23/IL-17-directed immunotherapy.

This study provides a framework for understanding the role that IL-23 plays in mediating the host response to *P. aeruginosa* infection. Although murine systems are useful in modeling human immune responses, the conclusions that we reach are limited by the inherent interspecies differences. Moreover, further limitations are imposed as CF knockout mice neither manifest chronic airway symptoms nor become chronically infected with respiratory pathogens as humans with CF do; thus conducting further studies focused on the immunology of chronic lung disease in CF knockout mice is of somewhat limited value. Also, these studies have not addressed the absolute requirement for IL-17 and IL-17F in mediating airway inflammation. These IL-17 family members, which are regulated by IL-23 and expressed by ThIL-17 cells (1,21,22), may be necessary intermediaries in IL-23-mediated neutrophil recruitment. It is with these limitations and conditions in mind that further studies of IL-23, IL-12p40, and IL-17 in murine models must be undertaken, the immunology literature from other disease states judiciously interpreted, and the observations in humans with CF synthesized to develop effective and safe immunotherapy.

Acknowledgments

We thank Nico Ghilardi at Genentech for providing the IL-23p19$^{-/-}$ mice for these studies. We also thank Dr. Anna van Heeckeren and the Animal Core at the Case Western Reserve University Cystic Fibrosis Center for the training and technical support provided in the agarose bead model of airway infection. In addition, we acknowledge Lauren Ulrich and Theresa Dubowski for technical assistance.

GRANTS

This work was supported by National Heart, Lung, and Blood Institute Grant R01-HL-079142.

References

1. Aggarwal S, Ghilardi N, Xie MH, de Sauvage FJ, Gurney AL. Interleukin-23 promotes a distinct CD4 T cell activation state characterized by the production of interleukin-17. J Biol Chem 2003;278:1910–1914. [PubMed: 12417590]
2. Armstrong DS, Hook SM, Jamsen KM, Nixon GM, Carzino R, Carlin JB, Robertson CF, Grimwood K. Lower airway inflammation in infants with cystic fibrosis detected by newborn screening. Pediatr Pulmonol 2005;40:500–510. [PubMed: 16208679]
3. Bonfield TL, Panuska JR, Konstan MW, Hilliard KA, Hilliard JB, Ghnaim H, Berger M. Inflammatory cytokines in cystic fibrosis lungs. Am J Respir Crit Care Med 1995;152:2111–2118. [PubMed: 8520783]
4. Brauner A, Cryz SJ, Granstrom M, Hanson HS, Lofstrand L, Strandvik B, Wretlind B. Immunoglobulin G antibodies to *Pseudomonas aeruginosa* lipopolysaccharides and exotoxin A in patients with cystic fibrosis or bacteremia. Eur J Clin Microbiol Infect Dis 1993;12:430–436. [PubMed: 8359163]
5. Carpagnano GE, Barnes PJ, Geddes DM, Hodson ME, Kharitonov SA. Increased leukotriene B4 and interleukin-6 in exhaled breath condensate in cystic fibrosis. Am J Respir Crit Care Med 2003;167:1109–1112. [PubMed: 12684249]
6. Chan SC, Shum DK, Ip MS. Sputum sol neutrophil elastase activity in bronchiectasis: differential modulation by syndecan-1. Am J Respir Crit Care Med 2003;168:192–198. [PubMed: 12702549]
7. Chmiel JF, Konstan MW, Saadane A, Krenicky JE, Lester Kirchner H, Berger M. Prolonged inflammatory response to acute *Pseudomonas* challenge in interleukin-10 knockout mice. Am J Respir Crit Care Med 2002;165:1176–1181. [PubMed: 11956064]
8. Cowan RG, Winnie GB. Anti-*Pseudomonas aeruginosa* IgG subclass titers in patients with cystic fibrosis: correlations with pulmonary function, neutrophil chemotaxis, and phagocytosis. J Clin Immunol 1993;13:359–370. [PubMed: 8245182]

9. Cua DJ, Sherlock J, Chen Y, Murphy CA, Joyce B, Seymour B, Lucian L, To W, Kwan S, Churakova T, Zurawski S, Wiekowski M, Lira SA, Gorman D, Kastelein RA, Sedgwick JD. Interleukin-23 rather than interleukin-12 is the critical cytokine for autoimmune inflammation of the brain. Nature 2003;421:744–748. [PubMed: 12610626]
10. Eigen H, Rosenstein BJ, FitzSimmons S, Schidlow DV. A multicenter study of alternate-day prednisone therapy in patients with cystic fibrosis. Cystic Fibrosis Foundation prednisone trial group. J Pediatr 1995;126:515–523. [PubMed: 7699528]
11. Fedele G, Stefanelli P, Spensieri F, Fazio C, Mastrantonio P, Ausiello CM. *Bordetella pertussis*-infected human monocyte-derived dendritic cells undergo maturation and induce Th1 polarization and interleukin-23 expression. Infect Immun 2005;73:1590–1597. [PubMed: 15731058]
12. Happel KI, Dubin PJ, Zheng M, Ghilardi N, Lockhart C, Quinton LJ, Odden AR, Shellito JE, Bagby GJ, Nelson S, Kolls JK. Divergent roles of IL-23 and IL-12 in host defense against *Klebsiella pneumoniae*. J Exp Med 2005;202:761–769. [PubMed: 16157683]
13. Happel KI, Zheng M, Young E, Quinton LJ, Lockhart E, Ramsay AJ, Shellito JE, Schurr JR, Bagby GJ, Nelson S, Kolls JK. Cutting edge: roles of Toll-like receptor 4 and IL-23 in IL-17 expression in response to *Klebsiella pneumoniae* infection. J Immunol 2003;170:4432–4436. [PubMed: 12707317]
14. Harrington LE, Hatton RD, Mangan PR, Turner H, Murphy TL, Murphy KM, Weaver CT. Interleukin 17-producing $CD4^+$ effector T cells develop via a lineage distinct from the T helper type 1 and 2 lineages. Nat Immunol 2005;6:1123–1132. [PubMed: 16200070]
15. Heinzel FP, Hujer AM, Ahmed FN, Rerko RM. In vivo production and function of IL-12 p40 homodimers. J Immunol 1997;158:4381–4388. [PubMed: 9127002]
16. Kersten CM, McCluskey RT, Shaw Warren H, Kurnick JT. Responses of human T cells to dominant discrete protein antigens of *Escherichia coli* and *Pseudomonas aeruginosa*. Scand J Immunol 1994;40:151–157. [PubMed: 7519358]
17. Khader SA, Pearl JE, Sakamoto K, Gilmartin L, Bell GK, Jelley-Gibbs DM, Ghilardi N, deSauvage F, Cooper AM. IL-23 compensates for the absence of IL-12p70 and is essential for the IL-17 response during tuberculosis but is dispensable for protection and antigen-specific IFN-gamma responses if IL-12p70 is available. J Immunol 2005;175:788–795. [PubMed: 16002675]
18. Kolls JK, Linden A. Interleukin-17 family members and inflammation. Immunity 2004;21:467–476. [PubMed: 15485625]
19. Konstan MW, Byard PJ, Hoppel CL, Davis PB. Effect of high-dose ibuprofen in patients with cystic fibrosis. N Engl J Med 1995;332:848–854. [PubMed: 7503838]
20. Lagace J, Peloquin L, Kermani P, Montie TC. IgG subclass responses to *Pseudomonas aeruginosa* a- and b-type flagellins in patients with cystic fibrosis: a prospective study. J Med Microbiol 1995;43:270–276. [PubMed: 7562988]
21. Langrish CL, Chen Y, Blumenschein WM, Mattson J, Basham B, Sedgwick JD, McClanahan T, Kastelein RA, Cua DJ. IL-23 drives a pathogenic T cell population that induces autoimmune inflammation. J Exp Med 2005;201:233–240. [PubMed: 15657292]
22. Langrish CL, McKenzie BS, Wilson NJ, de Waal Malefyt R, Kastelein RA, Cua DJ. IL-12 and IL-23: master regulators of innate and adaptive immunity. Immunol Rev 2004;202:96–105. [PubMed: 15546388]
23. Lubberts E. The role of IL-17 and family members in the pathogenesis of arthritis. Curr Opin Investig Drugs 2003;4:572–577.
24. McAllister F, Henry A, Kreindler JL, Dubin PJ, Ulrich L, Steele C, Finder JD, Pilewski JM, Carreno BM, Goldman SJ, Pirhonen J, Kolls JK. Role of IL-17A, IL-17F, and the IL-17 receptor in regulating growth-related oncogene-alpha and granulocyte colony-stimulating factor in bronchial epithelium: implications for airway inflammation in cystic fibrosis. J Immunol 2005;175:404–412. [PubMed: 15972674]
25. Muhlebach MS, Noah TL. Endotoxin activity and inflammatory markers in the airways of young patients with cystic fibrosis. Am J Respir Crit Care Med 2002;165:911–915. [PubMed: 11934713]
26. Muhlebach MS, Stewart PW, Leigh MW, Noah TL. Quantitation of inflammatory responses to bacteria in young cystic fibrosis and control patients. Am J Respir Crit Care Med 1999;160:186–191. [PubMed: 10390398]

27. Murphy CA, Langrish CL, Chen Y, Blumenschein W, McClanahan T, Kastelein RA, Sedgwick JD, Cua DJ. Divergent pro- and antiinflammatory roles for IL-23 and IL-12 in joint autoimmune inflammation. J Exp Med 2003;198:1951–1957. [PubMed: 14662908]

28. Noah TL, Murphy PC, Alink JJ, Leigh MW, Hull WM, Stahlman MT, Whitsett JA. Bronchoalveolar lavage fluid surfactant protein-A and surfactant protein-D are inversely related to inflammation in early cystic fibrosis. Am J Respir Crit Care Med 2003;168:685–691. [PubMed: 12829455]

29. Park H, Li Z, Yang XO, Chang SH, Nurieva R, Wang YH, Wang Y, Hood L, Zhu Z, Tian Q, Dong C. A distinct lineage of CD4 T cells regulates tissue inflammation by producing interleukin 17. Nat Immunol 2005;6:1133–1141. [PubMed: 16200068]

30. Porwoll JM, Gebel HM, Rodey GE, Markham RB. In vitro response of human T cells to *Pseudomonas aeruginosa*. Infect Immun 1983;40:670–674. [PubMed: 6404830]

31. Prikk K, Maisi P, Pirila E, Sepper R, Salo T, Wahlgren J, Sorsa T. In vivo collagenase-2 (MMP-8) expression by human bronchial epithelial cells and monocytes/macrophages in bronchiectasis. J Pathol 2001;194:232–238. [PubMed: 11400153]

32. Ratjen F, Hartog CM, Paul K, Wermelt J, Braun J. Matrix metalloproteases in BAL fluid of patients with cystic fibrosis and their modulation by treatment with dornase alpha. Thorax 2002;57:930–934. [PubMed: 12403873]

33. Ruddy MJ, Shen F, Smith JB, Sharma A, Gaffen SL. Interleukin-17 regulates expression of the CXC chemokine LIX/CXCL5 in osteoblasts: implications for inflammation and neutrophil recruitment. J Leukoc Biol 2004;76:135–144. [PubMed: 15107456]

34. Sagel SD, Kapsner RK, Osberg I. Induced sputum matrix metalloproteinase-9 correlates with lung function and airway inflammation in children with cystic fibrosis. Pediatr Pulmonol 2005;39:224–232. [PubMed: 15635615]

35. Sepper R, Konttinen YT, Ding Y, Takagi M, Sorsa T. Human neutrophil collagenase (MMP-8), identified in bronchiectasis BAL fluid, correlates with severity of disease. Chest 1995;107:1641–1647. [PubMed: 7781360]

36. Shum DK, Chan SC, Ip MS. Neutrophil-mediated degradation of lung proteoglycans: stimulation by tumor necrosis factor-alpha in sputum of patients with bronchiectasis. Am J Respir Crit Care Med 2000;162:1925–1931. [PubMed: 11069836]

37. Spensieri F, Fedele G, Fazio C, Nasso M, Stefanelli P, Mastrantonio P, Ausiello CM. *Bordetella pertussis* inhibition of interleukin-12 (IL-12) p70 in human monocyte-derived dendritic cells blocks IL-12 p35 through adenylate cyclase toxin-dependent cyclic AMP induction. Infect Immun 2006;74:2831–2838. [PubMed: 16622221]

38. van Heeckeren AM, Schluchter MD. Murine models of chronic *Pseudomonas aeruginosa* lung infection. Lab Anim 2002;36:291–312. [PubMed: 12144741]

39. van Heeckeren AM, Schluchter MD, Xue W, Davis PB. Response to acute lung infection with mucoid *Pseudomonas aeruginosa* in cystic fibrosis mice. Am J Respir Crit Care Med 2006;173:288–296. [PubMed: 16272448]

40. Ye P, Rodriguez FH, Kanaly S, Stocking KL, Schurr J, Schwarzen-berger P, Oliver P, Huang W, Zhang P, Zhang J, Shellito JE, Bagby GJ, Nelson S, Charrier K, Peschon JJ, Kolls JK. Requirement of interleukin 17 receptor signaling for lung CXC chemokine and granulocyte colony-stimulating factor expression, neutrophil recruitment, and host defense. J Exp Med 2001;194:519–527. [PubMed: 11514607]

41. Zheng L, Lam WK, Tipoe GL, Shum IH, Yan C, Leung R, Sun J, Ooi GC, Tsang KW. Overexpression of matrix metalloproteinase-8 and -9 in bronchiectatic airways in vivo. Eur Respir J 2002;20:170–176. [PubMed: 12166566]

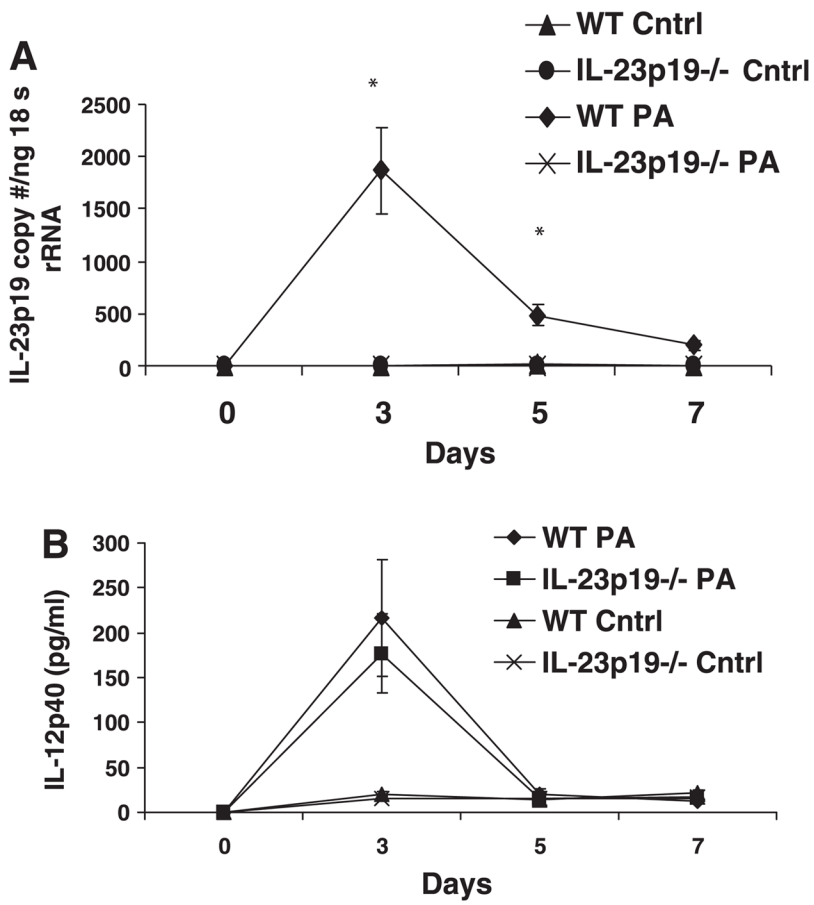

Fig. 1.

A: expression of IL-23p19 mRNA measured by TaqMan real-time PCR. Mice were killed after being infected with *Pseudomonas aeruginosa* strain PA M57–15-laden agarose beads for 0, 3, 5, and 7 days or uninfected control beads (Cntrl). IL-23p19$^{-/-}$ exhibited no detectable IL-23p19, whereas the wild-type (WT) infected mice had significantly increased IL-23p19 expression at *days 3* and *5*. There was no detectable IL-23p19 production in control mice. *B*: IL-12p40 was measured in the bronchoalveolar lavage (BAL) fluid at the protein level. There were no significant differences between infected WT and IL-23p19$^{-/-}$ mice. There is detectable production at baseline and for control mice of both groups and noted increase in IL-12p40 production in both WT and IL-23p19$^{-/-}$ mice at *day 3*. N = 3–5 per group for *A* and *B*.*P < 0.05.

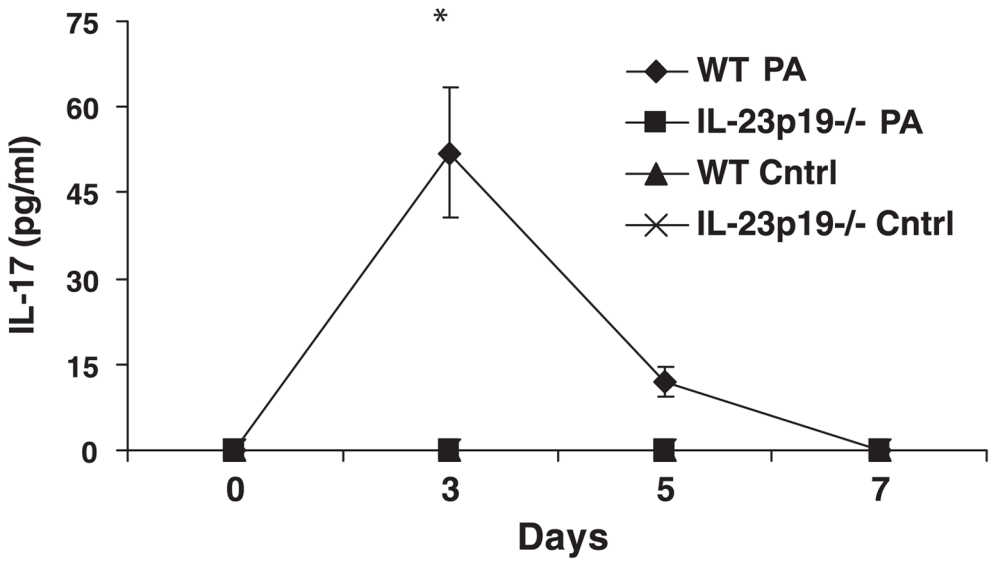

Fig. 2.

IL-17 protein measured by ELISA in BAL. IL-17 was measured at 0, 3, 5, and 7 days post-infection ($n = 5$ per group); $*P < 0.05$. IL-23p19$^{-/-}$ mice exhibited no detectable IL-17, whereas the WT infected mice had significantly increased IL-17 expression at *day 3*. IL-17 remained elevated at *day 5* in WT infected mice but was not significantly greater than the other groups. There was no detectable production of IL-17 in the WT or IL-23p19$^{-/-}$ control mice.

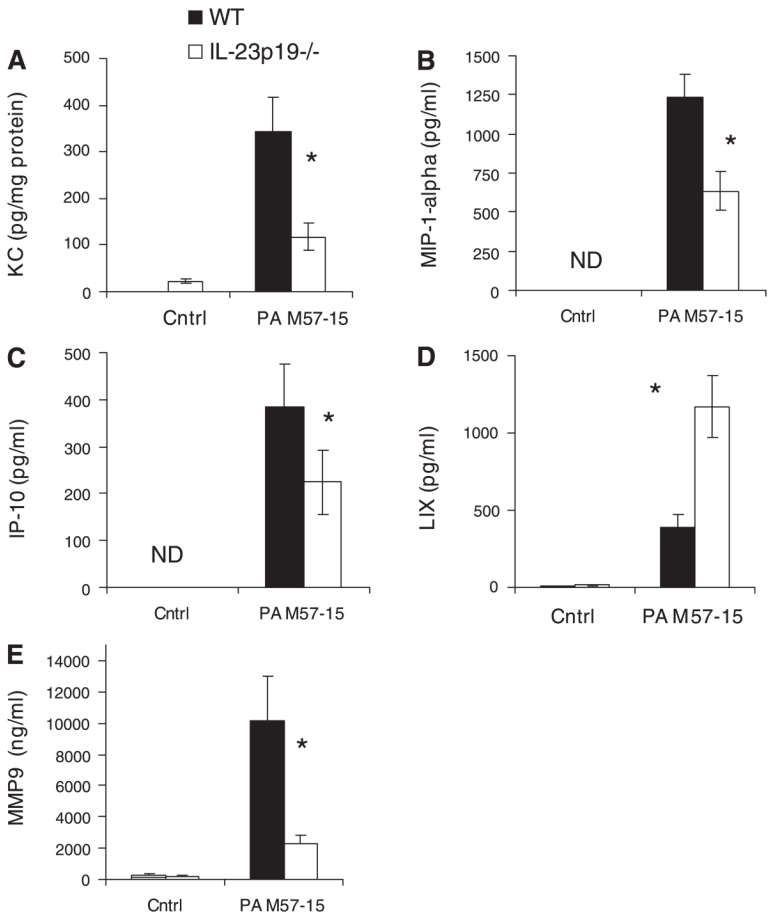

Fig. 3.

Chemokine and metalloproteinase (MMP) levels in lung homogenate and BAL fluid during chronic *P. aeruginosa* infection. Keratinocyte-derived chemokine (KC) (*A*) and MMP-9 (*E*) from lung homogenate were measured by LINCOplex and reported for *day 5* after infection ($n = 3–5$ per group); $*P < 0.05$. LPS-induced CXC chemokine (LIX) (*D*) from BAL was measured by ELISA and reported for *day 5* after infection ($n = 5$); $*P < 0.05$. Macrophage inflammatory protein-1α (MIP-1α) (*B*) and IFN-γ-inducible protein 10 (IP-10) (*C*) from BAL were measured by LINCOplex and reported for *day 5* after infection. ($n = 5$); $*P < 0.05$. Levels in the mice treated with control beads were either not detectable (ND) or not significantly different from baseline. In addition, WT controls were not significantly different from IL-23p19$^{-/-}$ controls.

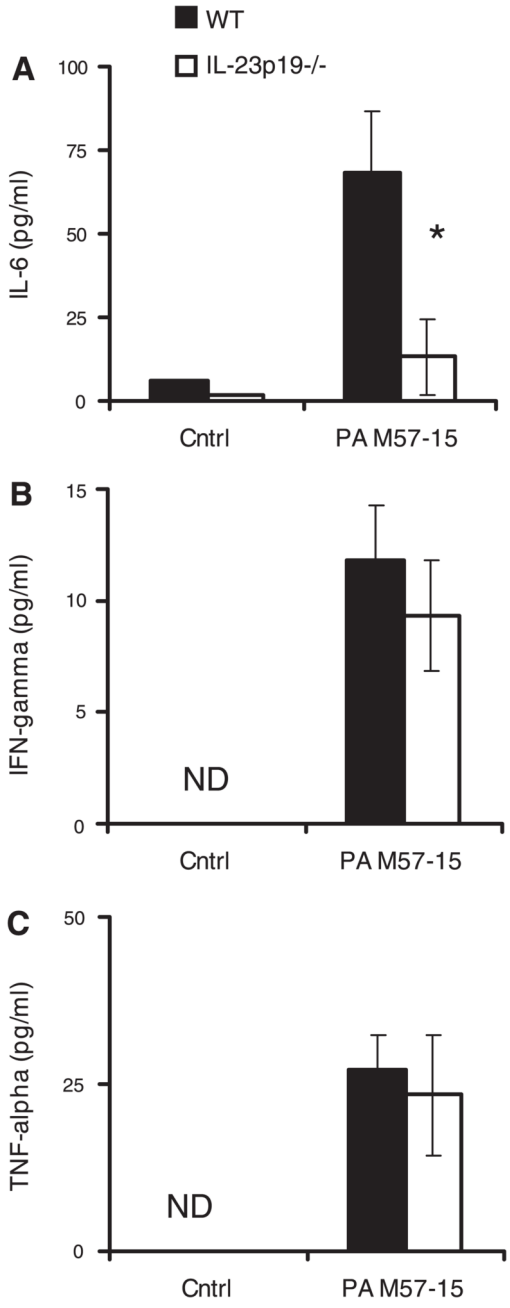

Fig. 4.

Cytokine levels in BAL fluid during chronic *P. aeruginosa* infection. IL-6 (*A*), IFN-γ (*D*), and TNF-α (*C*), measured by Luminex, are reported for *day 5* after infection. IL-6 was significantly increased in infected WT mice compared with IL-23p19$^{-/-}$ infected mice. Infected WT mice had significantly elevated levels over control WT mice. There was no significant difference between WT and IL-23p19$^{-/-}$ control mice ($n = 5$ per group); *$P < 0.05$.

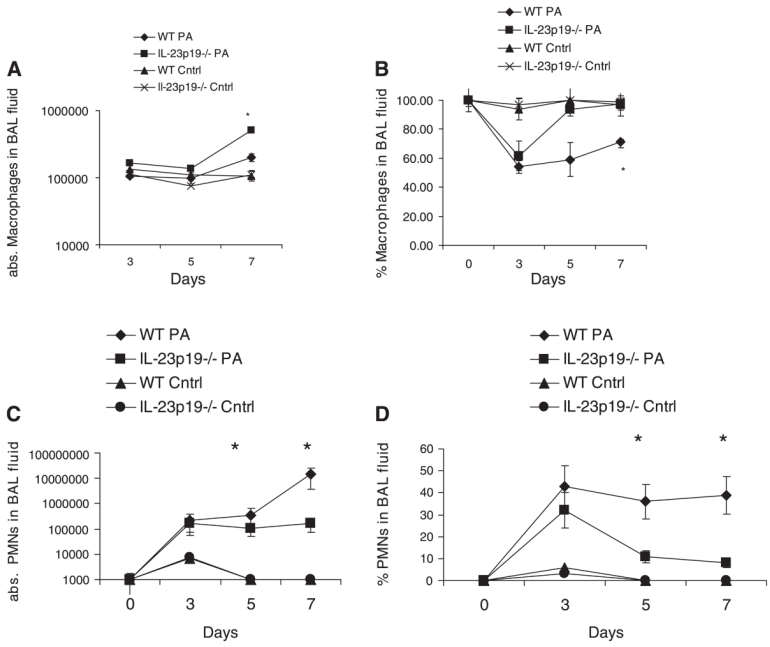

Fig. 5.

Cellular recruitment during chronic *P. aeruginosa* infection. *A*: absolute (abs.) numbers of recovered macrophages in BAL fluid from WT and IL-23p19$^{-/-}$ mice on *days 0*, *3*, *5*, and *7*. *B*: percent macrophages in BAL fluid from WT and IL-23p19$^{-/-}$ on *days 0*, *3*, *5*, and *7* after infection. *C*: absolute numbers of recovered neutrophils (PMNs) in BAL fluid from WT and IL-23p19$^{-/-}$ mice on *days 0*, *3*, *5*, and *7*. *D*: percent neutrophils in BAL fluid from WT and IL-23p19$^{-/-}$ mice on *days 0*, *3*, *5*, and *7* after infection. Where significant differences are noted, the infected WT mice demonstrate higher levels than the IL-23p19$^{-/-}$ infected mice and the WT control mice; there is no significant difference between WT and IL-23p19$^{-/-}$ control mice (n = 10 per group); *$P < 0.05$.

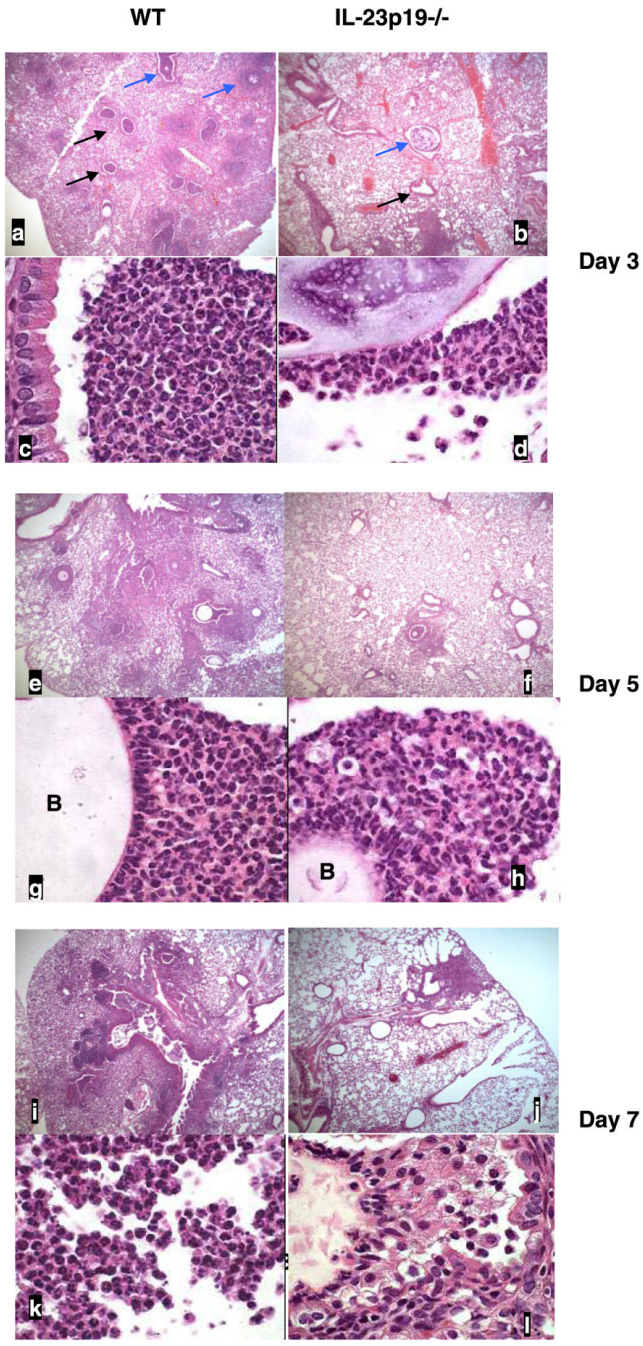

Fig. 6.

Representative photomicrographs of lung from WT and IL-23p19$^{-/-}$ mice infected with PA M57–15-laden beads at *days 3*, *5*, and *7*. *Top* panels for each time point are at ×50 magnification, and *bottom* panels are at ×1,000 magnification. *Day 3* (*a–d*): black arrows indicate airways with marked inflammation, and blue arrows indicate beads. *Day 5* (*e–h*): B marks agarose bead in the airway lumen. *i–l: day 7*.

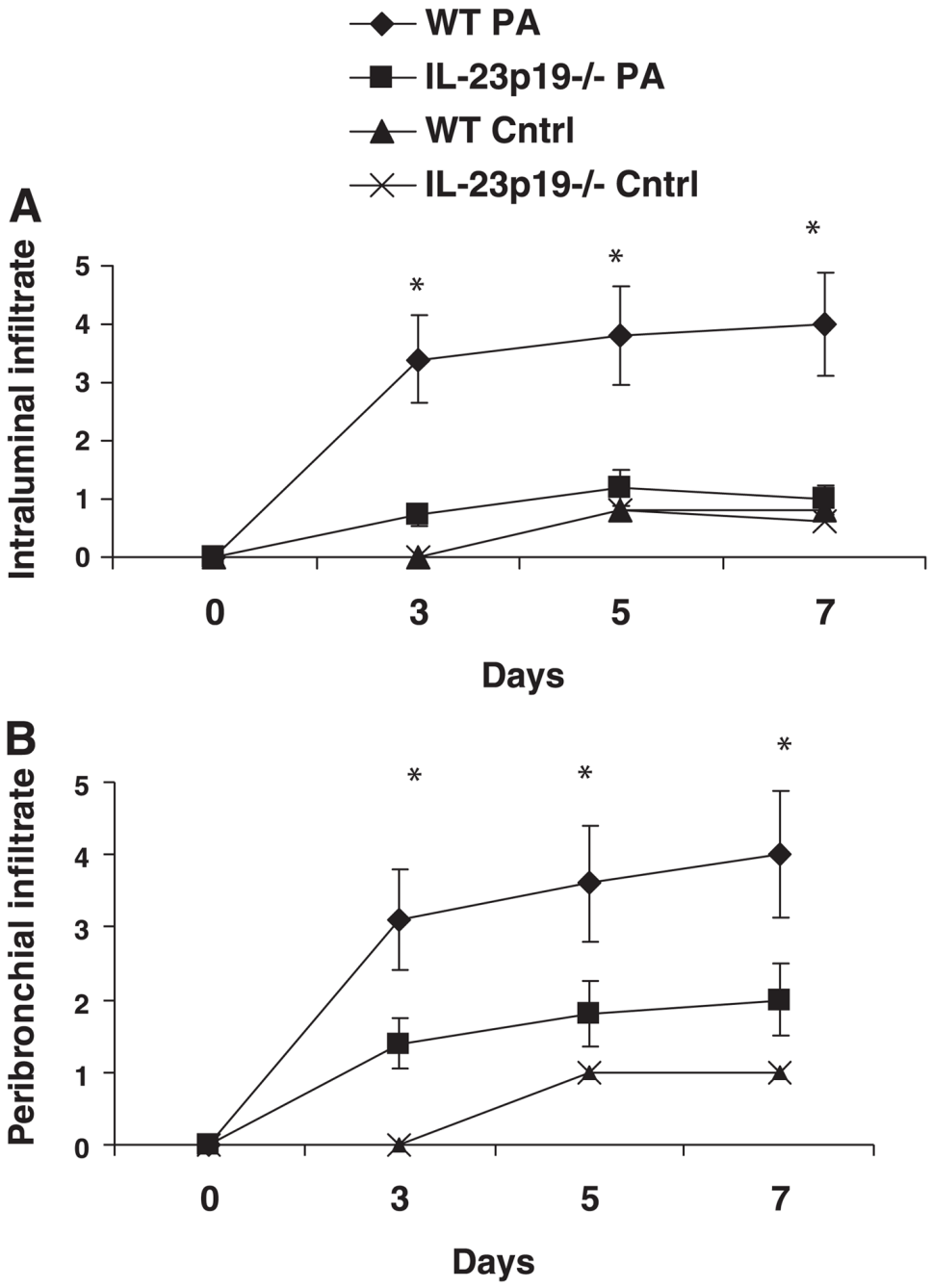

Fig. 7.

Quantitative scoring of intraluminal (*A*) and peribronchial (*B*) infiltrate: comparing WT and IL-23p19$^{-/-}$ infected and control demonstrates significant differences at *days 3*, *5*, and *7* for the infected WT mice compared with the IL-23p19$^{-/-}$ infected and WT control groups ($n = 5$ per group); *$P < 0.05$.

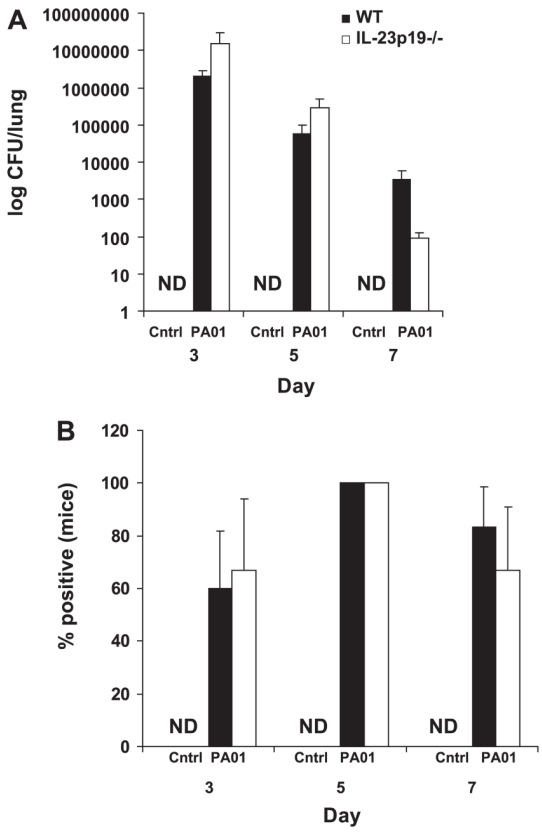

Fig. 8.

Quantitative comparisons of bacterial burden in the lung by comparison of colony-forming units (CFU) (*A*) and percent of mice originally infected from which bacteria are recovered (*B*) (*n* = per group).

Table 1

Histological scoring of inflammation in the lungs of wild-type (C57BL/6) and IL-23p19$^{-/-}$ mice infected with PA M57-15-laden beads

Score	Intraluminal Infiltrate	Peribronchial Infiltrate	Alveolar Involvement
0	None	None	None
1	≤25% of visualized lumens; predominate mononuclear	Infiltrate ≤4 cells thick	Increased cellularity; no evidence of septal thickening
2	25–50% of visualized lumens; mixed mono- and polymorphonuclear	Infiltrate 5–10 cells thick	Increased cellularity; evidence of septal thickening
3	50–75% of visualized lumens; predominately polymorphonuclear	25–50% visualized lumens	Significant cellularity, thickening; edema or blood; obliteration of <25% of visualized alveolar space
4	Diffuse; predominately polymorphonulcear	Diffuse	Obliteration of >25% of the alveolar space

Scores apply to microscopic fields at ×5 with visualized beads as evidence of involvement.